Electronic Supplementary Information

Increased chemical reactivity achieved by asymmetrical 'Janus' functionalisation of graphene

Mark A. Bissett,[†,§,*] Yuichiro Takesaki,[‡] Masaharu Tsuji,[†,‡] and Hiroki Ago[†,‡,‖]

[†]Institute for Materials Chemistry and Engineering (IMCE), Kyushu University, Fukuoka, 816-8580, Japan
[‡]Graduate School of Engineering Sciences, Kyushu University, Fukuoka, 816-8580, Japan
[‖]PRESTO, Japan Science and Technology Agency (JST), Saitama 332-0012, Japan
[§]Current address: Faculty of Engineering and Physical Sciences, School of Chemistry, University of Manchester, UK.

1. Experimental methods

Single-layer graphene was grown by ambient pressure chemical vapour deposition (CVD) on copper foil as published previously.[1] Briefly, copper foil (Alfa Aesar, 25 μm thick, 99.8% purity) was placed into a tube furnace with a 26 mm diameter quartz tube and annealed under a hydrogen (20 sccm) and argon (800 sccm) atmosphere at 1000 ^{O}C for 60 min, followed by graphene growth using methane (0.5 sccm) as the carbon source for 10 min, then cooled rapidly. Bilayer graphene was also synthesised by CVD using Cu-Ni alloy (Cu:Ni = 80:20) catalyst at 1000 ^{O}C. The addition of Ni in the Cu catalyst increased the carbon solubility, resulting in the formation of mono and few-layer graphene domains.

The graphene was then transferred from the copper foil to flexible PDMS substrates by drop coating liquid PDMS (Sylgard 184 Elastomer Kit, Dow Corning, USA), with a base to curing agent ratio of 10:1 before curing. After curing, the copper foil was removed by etching in 1M aqueous $FeCl_3$ leaving the graphene attached to the cured PDMS substrate. After transferring onto the PDMS the graphene was stamp transferred onto Si/SiO_2 wafers for functionalisation and analysis.[2,3]

Covalent diazonium functionalisation was then performed by submerging the Si/SiO_2 supported graphene substrates into aqueous solutions of 20 mM 4-nitrobenzenediazonium tetrafluoroborate (NBD, Tokyo Chemical Industry, Japan) or 4-methoxybenzenediazonium tetrafluoroborate (MBD) for 10 mins. To perform bifacial functionalisation the graphene was initially functionalised while still supported by the PDMS, and then the opposing face is functionalised after transfer to the Si/SiO_2 wafer. For the synthesis of Janus graphene, MBD was first reacted, followed by reaction of the opposing side with NBD after transferring onto the SiO_2 surface.

Raman spectroscopy was performed on a Nanofinder 30 (Tokyo Instruments, Japan) using a laser excitation wavelength of 532 nm with a power of 1 mW and a 100× objective with a numerical aperture of 0.9. Raman maps were constructed by taking spectra spaced by 300 nm.

2. Chemical structures of functionalised monolayer and bilayer graphene

(a) Monolayer graphene

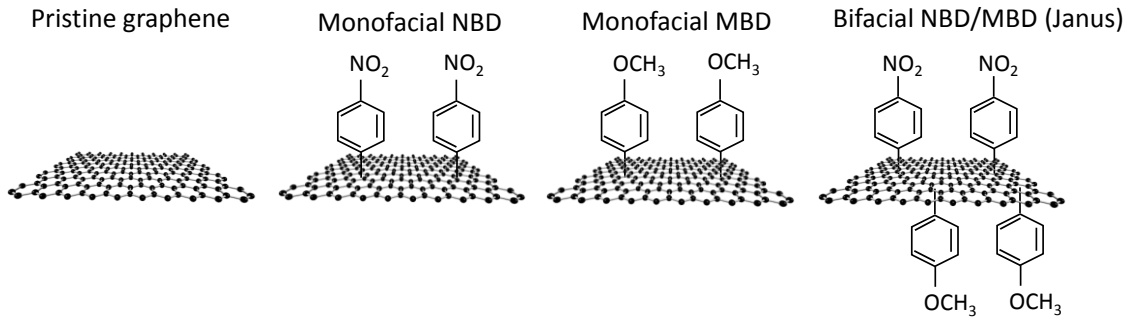

(b) Bilayer graphene

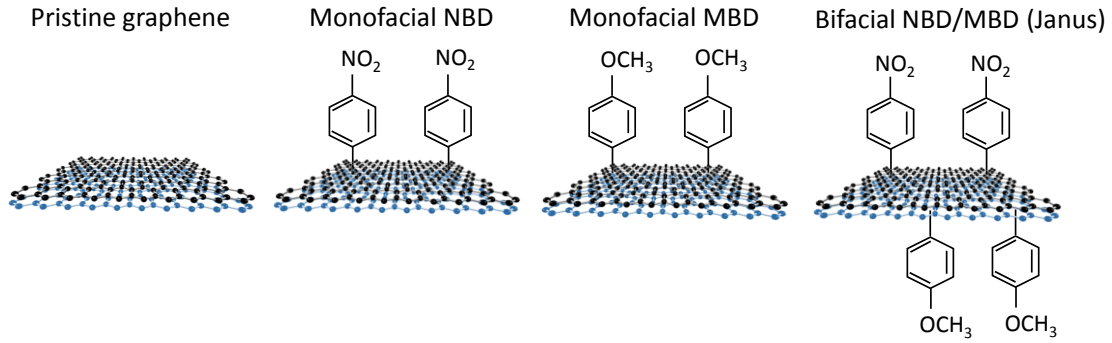

Figure SI-1: Schematic chemical structures of functionalised graphene shown in Figure 2 of the main text.

3. Doping of graphene by aryl diazonium molecules

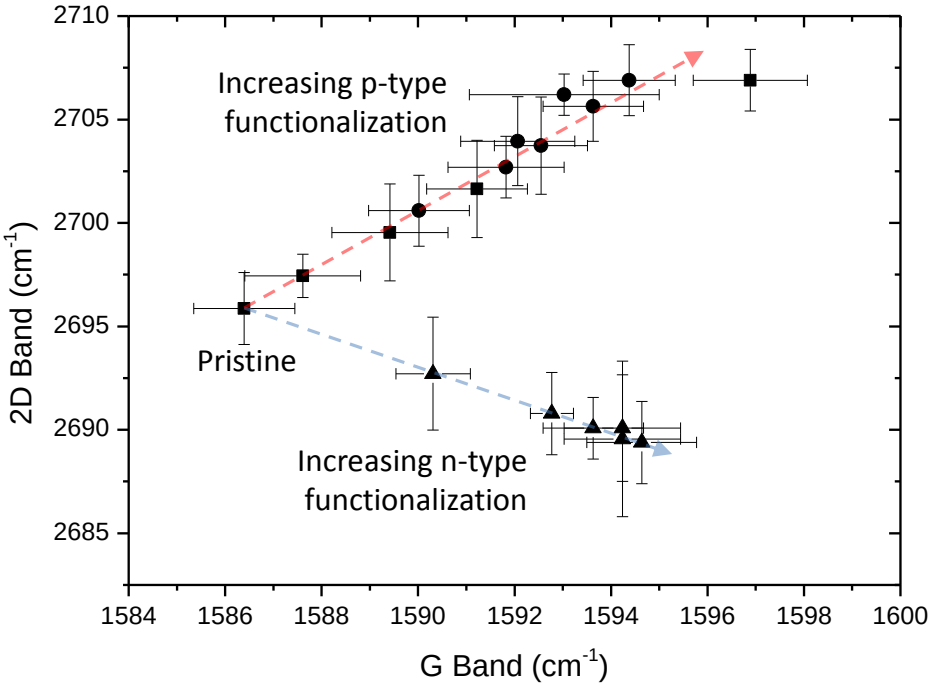

Figure SI-2: Plot of 2D peak frequency versus G band frequency for pristine and diazonium functionalised graphene. With increasing NBD functionalisation time we observe an increase in both the G and 2D band frequency, indicating p-type doping. While with increasing MBD functionalisation time we see an increase in G band frequency but a decrease in the 2D frequency, indicating n-type doping. This matches the results achieved through electrochemical gating of graphene.[4-7] Previous work on the chemical doping of graphene oxide has shown a different trend due to the starting material not being pristine.[8] The data presented in Fig. SI-2 is of graphene still supported on copper foil and thus the frequencies are upshifted as expected due to substrate interactions[9] for the pristine and all subsequent functionalisation times.

4. Raman parameters after functionalisation

Monolayer

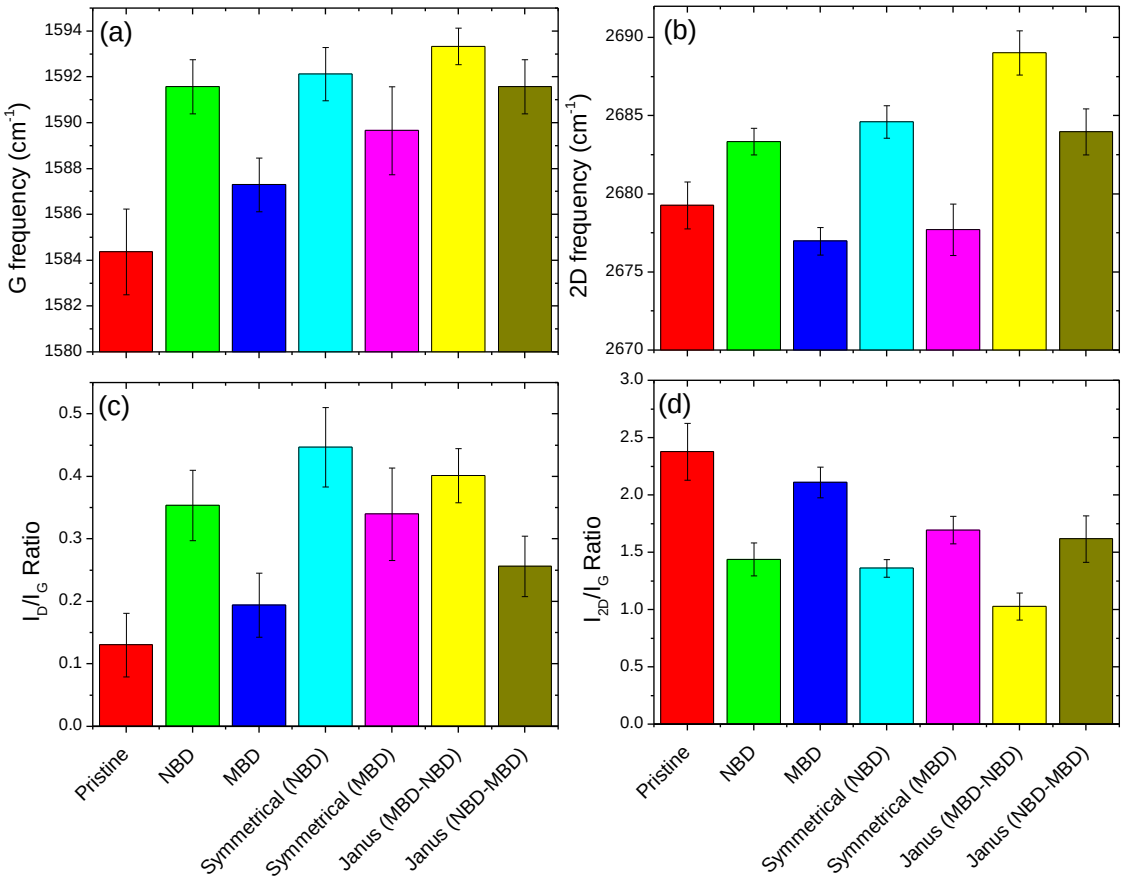

Figure SI-3: Column graphs comparing the Raman peak parameters for all examined monolayer graphene functionalisation schemes. The error bars represent one standard deviation. **(a)** Plot of G peak frequency showing that after functionalisation that the frequency increases for all doping, in agreement with results from electrochemically gated graphene.[4,6,7] The magnitude of peak shift is proportional to level of doping and thus we can clearly see that the NBD dopes the graphene much more than the MBD due to higher reactivity. The symmetrical bifacial functionalisation increases the level of doping only marginally from the single sided functionalisation, suggesting that simply increasing the available attachment sites cannot significantly increase the level of doping. While the Janus graphene functionalised by MBD followed by NBD (Janus MBD-NBD) shows the highest level of doping indicating that its level of functionalisation was also the highest. **(b)** Plot of 2D frequency for each functionalisation scheme. As we have seen in Fig. S2 an increase in the 2D frequency is indicative of p-type doping, while a decrease indicates n-type doping. From this we can see that NBD and the Janus functionalisation causes p-type doping while MBD causes n-type doping, but to a lesser magnitude. **(c, d)** The plot of the I_D/I_G and I_{2D}/I_G ratios agree with the peak position results that show increased levels of covalent functionalisation, represented by an increased I_D/I_G ratio, correspond to increased doping. The I_{2D}/I_G ratio decreases with increasing functionalisation due to charge transfer and thus the largest decrease occurs for the Janus graphene.

Bilayer

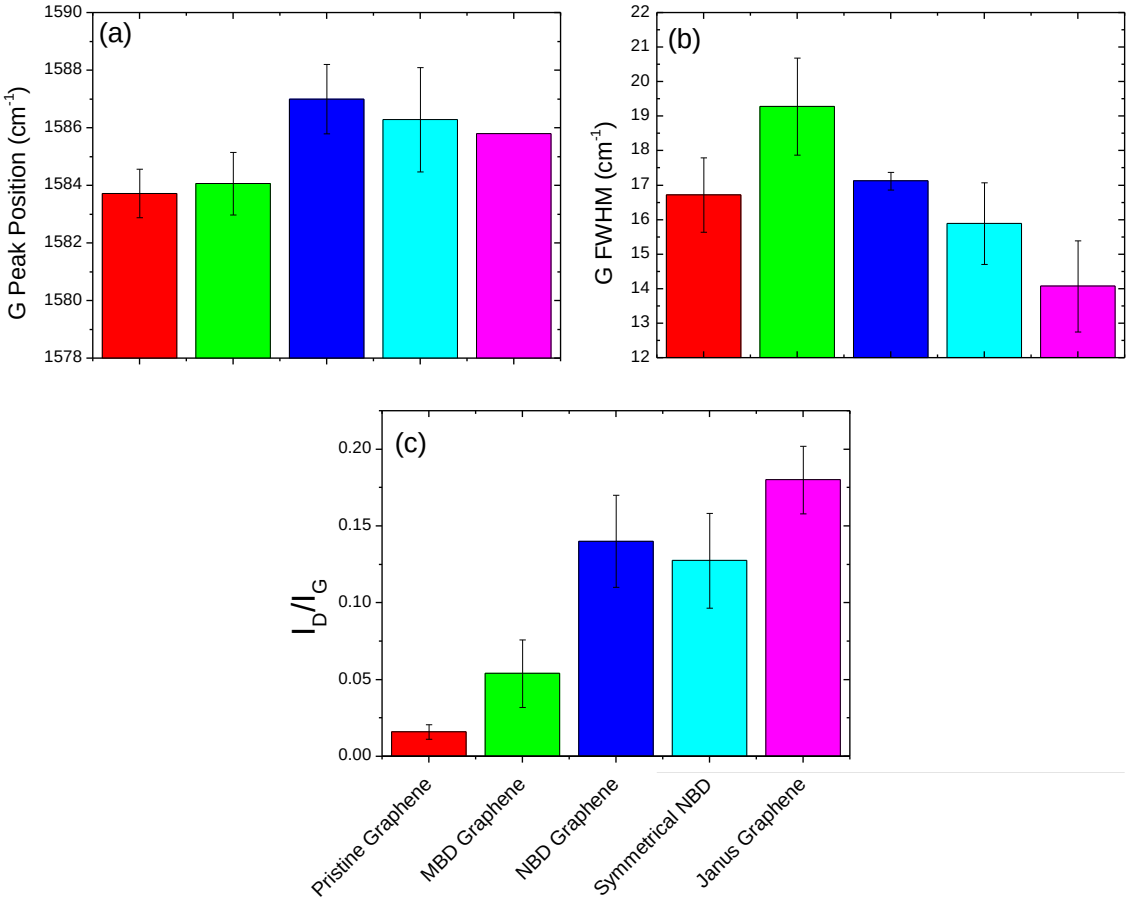

Figure SI-4: Column graphs comparing the Raman peak parameters for all examined bilayer graphene functionalisation schemes. The error bars represent one standard deviation. **(a)** Plot of G peak frequency showing that after functionalisation that the frequency increases for the NBD, MBD, symmetrical and Janus schemes. Previous work on the diazonium functionalisation of bilayer graphene showed the opposite behaviour than we have shown here, with a decrease in G peak frequency for a p-type dopant,[10] however no clear reason explanation of this behaviour is provided. Electrochemically gated bilayer graphene has been found to behave in a similar fashion to monolayer,[11] and this same trend is observed here. **(b)** The FWHM of the G band in bilayer graphene was found to increase for n-type doping, but decrease for increasing p-type doping. This again is different from the behaviour observed in gated graphene[11] and may be related to the presence of covalent attachment sites occurring on only one of the layers a opposed to an externally applied electric field. **(c)** Plot of I_D/I_G ratio shows the same trend as observed for monolayer graphene of an increase for each covalent attachment scheme, with the smallest increase for the MBD and the largest for the Janus functionalisation. Of note is that again the Janus functionalisation shows a significant increase over the symmetrical NBD functionalisation, indicating that the use of asymmetrical functionalisation can achieve higher degrees of functionalisation.

5. Further Raman maps

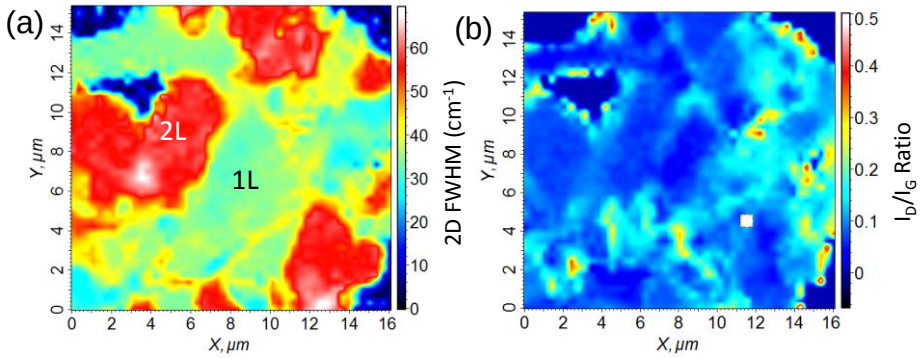

Figure SI-5: Raman maps of 2D FWHM (a) and I_D/I_G ratio (b) for pristine graphene showing areas of bilayer as well as monolayer.

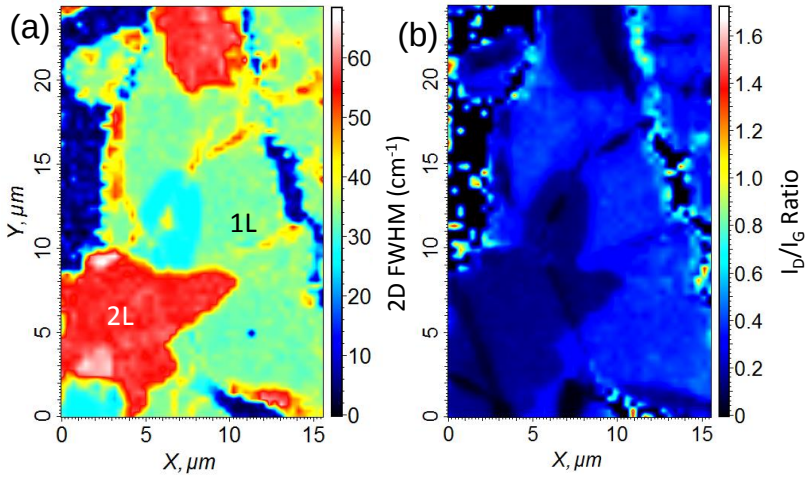

Figure SI-6: Raman maps of 2D FWHM (a) and I_D/I_G ratio (b) for monofacially NBD functionalised graphene showing areas of bilayer as well as monolayer.

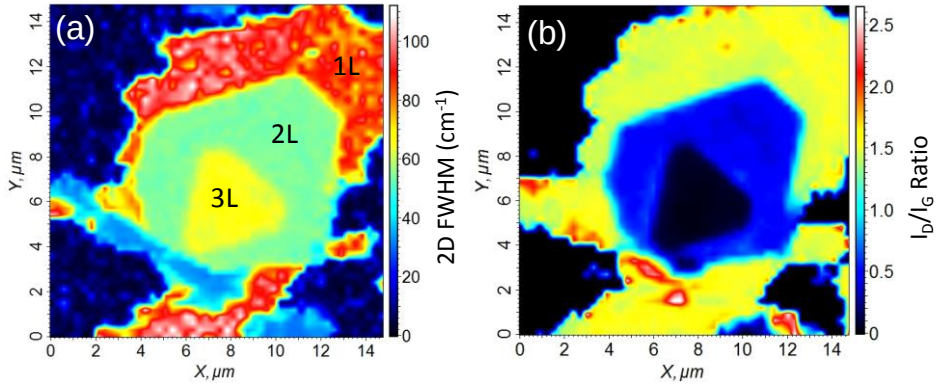

Figure SI-7: Raman maps of 2D FWHM (a) and I_D/I_G ratio (b) for Janus functionalised graphene showing areas of bilayer as well as monolayer. The width (a) of the 1L region is increased drastically after the Janus functionalisation due to the higher chemical reactivity of monolayer graphene compared to the 2L and 3L regions.

Supporting References

1. C. M. Orofeo, H. Hibino, K. Kawahara, Y. Ogawa, M. Tsuji, K.-i. Ikeda, S. Mizuno and H. Ago, *Carbon*, 2012, **50**, 2189-2196.
2. S. J. Kang, B. Kim, K. S. Kim, Y. Zhao, Z. Chen, G. H. Lee, J. Hone, P. Kim and C. Nuckolls, *Adv. Mater.*, 2011, **23**, 3531-3535.
3. J. Song, F.-Y. Kam, R.-Q. Png, W.-L. Seah, J.-M. Zhuo, G.-K. Lim, P. K. H. Ho and L.-L. Chua, *Nat. Nanotechnol.*, 2013, **8**, 356-362.
4. A. Das, S. Pisana, B. Chakraborty, S. Piscanec, S. K. Saha, U. V. Waghmare, K. S. Novoselov, H. R. Krishnamurthy, A. K. Geim, A. C. Ferrari and A. K. Sood, *Nat. Nanotechnol.*, 2008, **3**, 210-215.
5. D. M. Basko, S. Piscanec and A. C. Ferrari, *Phys. Rev. B*, 2009, **80**, 165413.
6. S. Pisana, M. Lazzeri, C. Casiraghi, K. S. Novoselov, A. K. Geim, A. C. Ferrari and F. Mauri, *Nat. Mater.*, 2007, **6**, 198-201.
7. M. Lazzeri and F. Mauri, *Phys. Rev. Lett.*, 2006, **97**, 266407.
8. M. A. Bissett, M. Tsuji and H. Ago, *Phys. Chem. Chem. Phys*, 2014, **16**, 11124-11138.
9. R. He, L. Zhao, N. Petrone, K. S. Kim, M. Roth, J. Hone, P. Kim, A. Pasupathy and A. Pinczuk, *Nano Lett.*, 2012, **12**, 2408-2413.
10. Q. H. Wang, C.-J. Shih, G. L. C. Paulus and M. S. Strano, *J. Am. Chem. Soc.*, 2013, **135**, 18866-18875.
11. A. Das, B. Chakraborty, S. Piscanec, S. Pisana, A. K. Sood and A. C. Ferrari, *Phys. Rev. B*, 2009, **79**, 155417.